

Energy dependence of the cross sections for the  $^{24}\text{Mg}(^{16}\text{O}, ^{12}\text{C})^{28}\text{Si}(\text{g.s.})$  reaction

S. J. Sanders

*A. W. Wright Nuclear Structure Laboratory, Yale University, New Haven, Connecticut 06511  
and Argonne National Laboratory, Argonne, Illinois 60439*H. Ernst,\* W. Henning, C. Jachcinski,† D. G. Kovar, and J. P. Schiffer  
*Argonne National Laboratory, Argonne, Illinois 60439*

J. Barrette‡

*Brookhaven National Laboratory, Upton, New York 11973*

(Received 10 December 1984)

Excitation functions have been measured at  $0^\circ$  and  $180^\circ$  for the  $^{24}\text{Mg}(^{16}\text{O}, ^{12}\text{C})^{28}\text{Si}(\text{g.s.})$  reaction, and at  $180^\circ$  for the  $^{24}\text{Mg}(^{16}\text{O}, ^{12}\text{C})^{28}\text{Si}(2^+)$  reaction over the energy range  $36 \text{ MeV} \leq E_{\text{c.m.}} \leq 54 \text{ MeV}$ . Angular distributions were measured at  $E_{\text{c.m.}} = 35.5$  and  $36.2 \text{ MeV}$  where, for the latter energy, much of the angular range between  $0^\circ$  and  $180^\circ$  was covered. These data, combined with earlier measurements at lower energies, establish that the reaction cross section is strongly influenced by resonances of the compound system over a large energy range. At the higher energies, however, both the energy averaged cross section and the resonance amplitudes fall off sharply. An attempt is made to reproduce the observed structure in the  $^{28}\text{Si}(\text{g.s.})$   $0^\circ$  and  $180^\circ$  excitation functions by fitting to the data a band of Breit-Wigner resonances with an energy dependence proportional to  $J(J+1)$ . The general behavior of the  $0^\circ$  and  $180^\circ$  yield is well reproduced by this procedure, even though there are twice as many resonance poles as there are clear bumps in the data. Some regularity is evident in the resulting resonance parameters, although the fitted resonance amplitudes show greater scatter than expected for a nuclear molecular band.

## I. INTRODUCTION

The angular and energy dependence of the  $^{24}\text{Mg}(^{16}\text{O}, ^{12}\text{C})^{28}\text{Si}$  reaction has been the subject of a number of experiments, with recent interest focusing on the energy dependence of the cross section. Although the angular distributions at forward angles can be reproduced assuming a direct alpha-particle transfer mechanism within a standard DWBA framework,<sup>1,2</sup> such calculations cannot reproduce the pronounced structures observed in excitation functions.<sup>3,4</sup> Considerable data relevant to this reaction have been accumulated. These include forward-angle excitation functions for the reaction leading to the ground state and a number of excited states of  $^{28}\text{Si}$  with  $E_x(^{28}\text{Si}) < 10 \text{ MeV}$ ,<sup>3,5-7</sup> excitation functions of the transitions to the  $^{28}\text{Si}$  ground state and first excited state<sup>8-11</sup> measured at  $180^\circ$ , and excitation functions of the  $180^\circ$  elastic scattering yields in both the entrance  $^{16}\text{O} + ^{24}\text{Mg}$  (Refs. 8 and 11) and exit  $^{12}\text{C} + ^{28}\text{Si}$  (Refs. 12 and 13) channels.

Most of these excitation function studies have been limited to the energy range of the Coulomb barrier to about twice the barrier energy. The excitation functions are found to exhibit gross structures of widths  $\Gamma \sim 1-2 \text{ MeV}$  and, where the experimental energy resolution permits, these gross structures are found to be further fragmented into intermediate structures of width  $\Gamma < 1 \text{ MeV}$ .<sup>7,14</sup> The widths and cross sections of these resonances depend on overlaps with the entrance and exit channels and with other open channels, including the spreading of the configu-

ration among states of the compound nucleus. At higher energies the competition with direct quasielastic and deep inelastic scattering may become more important as these processes become dominant for near grazing collisions. The overall trend of the data indicates a decreasing yield to the  $^{12}\text{C} + ^{28}\text{Si}(\text{g.s.})$  channel as the center of mass energy increases above  $\sim 32 \text{ MeV}$  for the  $^{16}\text{O} + ^{24}\text{Mg}$  system.

This paper reports on an extension of the  $^{24}\text{Mg}(^{16}\text{O}, ^{12}\text{C})^{28}\text{Si}$  excitation function at  $0^\circ$  and  $180^\circ$  to  $E_{\text{c.m.}} = 53 \text{ MeV}$  (about three times the Coulomb barrier). Two measurements which overlap and complement the present ones are excitation functions at  $\theta_{\text{lab}} = 5^\circ$  for  $32 \text{ MeV} < E_{\text{c.m.}} < 49 \text{ MeV}$  of  $^{24}\text{Mg}(^{16}\text{O}, ^{12}\text{C})^{28}\text{Si}(\text{g.s.}; 2^+)$  reactions by Nurzynski *et al.*,<sup>6</sup> and excitation functions measured by Braun-Munzinger *et al.*<sup>15</sup> of the  $^{12}\text{C} + ^{28}\text{Si}$  elastic and inelastic scattering channels at  $180^\circ$  covering the range  $14 \text{ MeV} \leq E_{\text{c.m.}} \leq 52 \text{ MeV}$ .

The details of the experimental measurements are discussed in Sec. II, and the results are presented. In Secs. III and IV there are separate discussions of the significant features of the forward and backward angle results. A general analysis of the combined forward and backward angle data follows in Sec. V, and a discussion as to what these data imply for a molecular resonance interpretation of the scattering process is presented in Sec. VI.

## II. EXPERIMENTAL ARRANGEMENT

The zero-degree excitation function for the  $^{24}\text{Mg}(^{16}\text{O}, ^{12}\text{C})^{28}\text{Si}$  reaction was measured with 60

$\text{MeV} \leq E_{\text{lab}}(^{16}\text{O}) \leq 90$  MeV using a beam from the Argonne superconducting linac. A differential absorption technique was used with the  $^{12}\text{C}$  particles identified in a Si (surface-barrier)  $\Delta E$ - $E$  telescope ( $\Omega=9.3$  msr) located behind a Au foil. The primary  $^{16}\text{O}$  beam was stopped in the Au foil. A schematic drawing of the experimental arrangement is shown in Fig. 1. The positive  $Q$  value for the reaction ( $Q_0=2.82$  MeV) allowed for clean identification of the  $^{28}\text{Si}(\text{g.s.})$  transition, although excited state transitions could not be resolved from other reaction products produced in the target and the absorber foil. The maximum energy to which the excitation function could be extended by this technique was set by the intense flux of reaction products obtained when the beam energy exceeded the Coulomb barrier for scattering of  $^{16}\text{O}$  on Au [corresponding to  $E_{\text{lab}}(^{16}\text{O}) \approx 82$  MeV].

The relative normalization of the yield at each energy was accomplished by monitoring the  $^{16}\text{O}$  ions backscattered from the Au absorber in a Si(SB) detector located at  $135^\circ$ . A calculated thick target spectrum (using  $^{16}\text{O} + ^{197}\text{Au}$  scattering cross sections obtained from an optical model calculation folded into the stopping power values given by Northcliffe and Schilling<sup>16</sup>) was scaled to the measured spectrum to obtain a normalization factor. The insert in Fig. 1 indicates the general qualitative behavior of the backscattered spectrum. Self-supporting  $^{24}\text{Mg}$  targets of approximately  $150 \mu\text{g}/\text{cm}^2$  area density were used in these measurements. It was assumed that there were no substantial changes in the  $^{24}\text{Mg}$  target thickness over the course of the experiment. Previous experience with similar targets has shown that these targets can withstand substantial beam currents ( $\sim 40$  particle nA) over extended periods of time without changing thickness or becoming seriously degraded.

After the relative normalization was established, the present excitation function was scaled to match with the lower energy data of Paul *et al.*<sup>3</sup> at common energies. Considering the uncertainty in the absolute normalization of the previously measured  $0^\circ$  data ( $\sim 25\%$ ), together

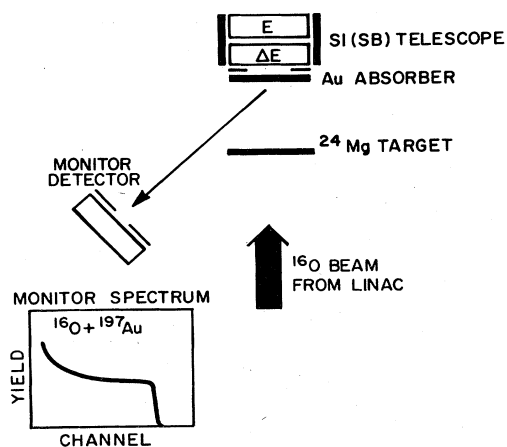


FIG. 1. Schematic of the experimental arrangement. The general shape of the monitor energy spectrum of backscattered  $^{16}\text{O}$  ions from the Au absorber is indicated.

with the uncertainty in this matching procedure, the uncertainty in the absolute normalization of the new data is estimated as  $\sim 35\%$ . In Fig. 2 the present excitation function along with the previously measured data are shown. Systematic uncertainties are not included in the error bars. All of the data in Fig. 2 have been corrected for energy losses in the target.

Angular distributions at  $E_{\text{c.m.}} = 35.5$  and  $36.2$  MeV for the  $^{24}\text{Mg}(^{16}\text{O}, ^{12}\text{C})^{28}\text{Si}(\text{g.s.})$  reaction were also measured at forward angles as shown in Fig. 3. These data were obtained using a  $\Delta E$ - $E$  Si(SB) telescope with a  $1^\circ$  angular acceptance, and were normalized by measuring forward angle elastic scattering in a monitor detector.

The  $180^\circ$  excitation functions for the reactions  $^{24}\text{Mg}(^{16}\text{O}, ^{12}\text{C})^{28}\text{Si}(\text{g.s.}; 2^+)$ ,  $1.78$  MeV) were measured at  $36 \text{ MeV} \leq E_{\text{c.m.}} \leq 54$  MeV in 300 steps using the same technique as discussed in Ref. 11, where the energy range  $24 \text{ MeV} \leq E_{\text{c.m.}} \leq 38$  MeV was covered. Beams of  $^{24}\text{Mg}$  in the energy range  $90 \text{ MeV} \leq E_{\text{lab}}(^{24}\text{Mg}) \leq 135$  MeV were obtained from the Brookhaven National Laboratory (BNL) tandem Van de Graaff facility. These beams were incident on self-supporting  $\text{Al}_2\text{O}_3$  targets, about  $100 \mu\text{g}/\text{cm}^2$  in areal density, and the outgoing  $^{12}\text{C}$  particles were detected at zero degree in the BNL quadrupole-dipole-dipole-dipole (QDDD) magnetic spectrometer equipped with a double-wire proportional counter. The square-shaped spectrometer aperture subtended in-plane angles of  $\pm 3^\circ$ . The primary  $^{24}\text{Mg}$  beam was stopped before the counter in a combination of gold and Havar absorber foils. The yields were normalized to the  $^{24}\text{Mg} + ^{27}\text{Al}$  elastic scattering yields detected in two monitor detectors, which were symmetrically located out-of-plane at  $18^\circ$  with respect to the beam. At  $E_{\text{lab}}(^{24}\text{Mg}) = 114.75$ , an angular distribution was measured for the  $^{12}\text{C}$  yield with  $0^\circ \leq \theta_{\text{lab}} \leq 12.8^\circ$ . For this angular distri-

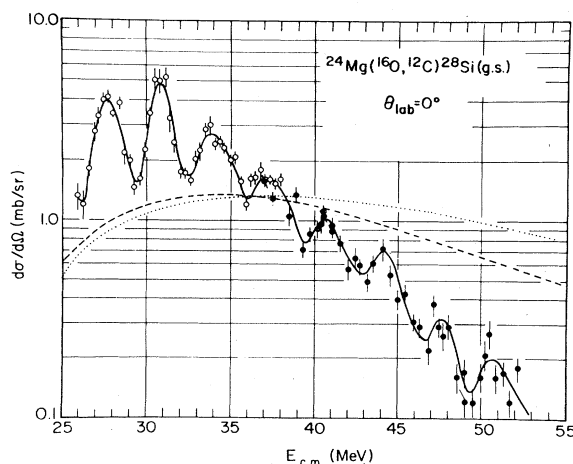


FIG. 2. Excitation function for the  $^{24}\text{Mg}(^{16}\text{O}, ^{12}\text{C})^{28}\text{Si}(\text{g.s.})$  reaction obtained at  $0^\circ$ . The closed points are the new results. The open circles are from Ref. 3. The solid curve is to guide the eye. The dotted and dashed curves represent typical results of DWBA calculations; these curves were calculated using the ANL1 and ANL2 potentials quoted in Ref. 4, respectively.

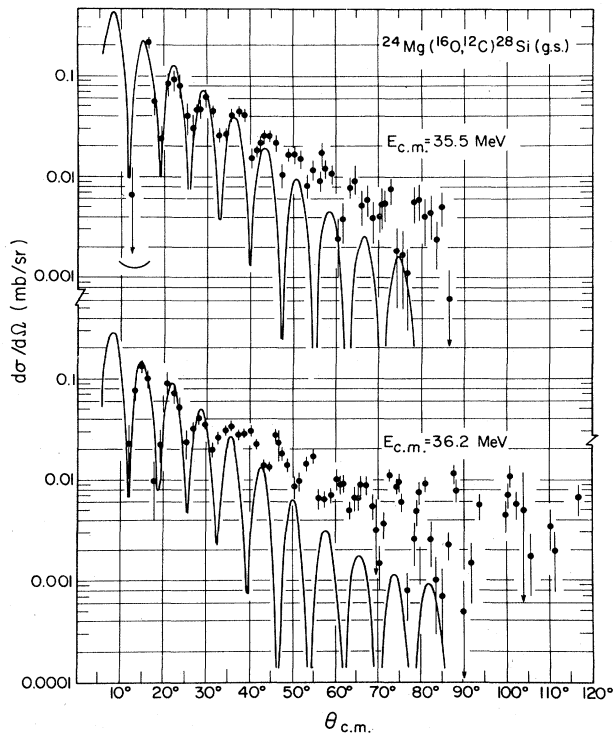


FIG. 3. Angular distribution measurements for the  $^{24}\text{Mg}(^{16}\text{O}, ^{12}\text{C})^{28}\text{Si}(\text{g.s.})$  reaction at  $E_{\text{c.m.}} = 35.5$  and  $36.2$  MeV. The curves are the results of DWBA calculations as discussed in the text.

bution the spectrometer aperture subtended in-plane angles of  $\pm 0.5^\circ$ . Further details can be found in Ref. 11. The excitation function data are shown, together with the lower energy measurements of Ref. 11, in Fig. 4. The angular distribution data are shown at the bottom of Fig. 6.

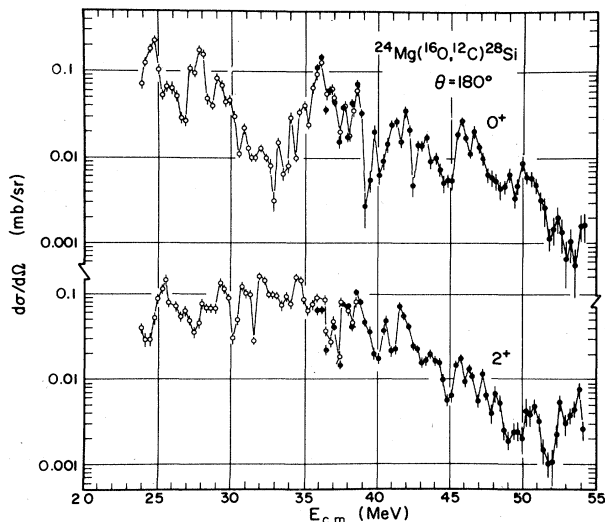


FIG. 4. Excitation functions measured at  $180^\circ$  for the  $^{24}\text{Mg}(^{16}\text{O}, ^{12}\text{C})^{28}\text{Si}$  reaction going to the ground state and ( $2^+$ ;  $1.78$  MeV) state in  $^{28}\text{Si}$ . The closed points are the new results. The open circles are from Ref. 11.

### III. FORWARD-ANGLE MEASUREMENTS

Perhaps the most remarkable feature evident in the  $^{24}\text{Mg}(^{16}\text{O}, ^{12}\text{C})^{28}\text{Si}(\text{g.s.})$  excitation function at  $0^\circ$  is the apparent regularity of the observed structures. In Fig. 2, a smooth curve is drawn through the data to suggest eight structures in the energy range covered. A regular behavior for the energy spacing might be expected in a simple molecular cluster model where the structures correspond to different molecular states in the compound system and are characterized by spin angular momentum  $J$  following a  $J(J+1)$  rotational energy sequence.<sup>17</sup> Problems with this very simple model are immediately evident, however. Experimentally there is no observed systematic increase in the spacing as a function of energy, in contrast to the behavior expected from a  $J(J+1)$  dependence. The structures have a mean spacing of  $\sim 3.2$  MeV with a variance of  $0.21$  MeV. Also, the spacing of clear resonant bumps in the cross section is approximately twice that expected for a  $^{16}\text{O} + ^{24}\text{Mg}$  nuclear molecule.<sup>18</sup> It seems unlikely, then, that the forward angle data can be described simply in terms of a rotational band of *nonoverlapping* resonances. A more detailed analysis with *overlapping* resonances is described in Sec. VI.

As has been noted previously,<sup>1,2</sup> isolated angular distributions of the  $^{24}\text{Mg}(^{16}\text{O}, ^{12}\text{C})^{28}\text{Si}(\text{g.s.})$  reaction at forward angles can be fitted by DWBA calculations. Such calculations are included in Fig. 3 for angular distributions measured at  $E_{\text{c.m.}} = 35.5$  and  $36.2$  MeV. These energies are both near a minimum in the zero-degree excitation function, although at  $36.2$  MeV there is a strong maximum in the  $180^\circ$  excitation function. At the most forward angles,  $\theta_{\text{c.m.}} < 30^\circ$ , the calculations reproduce the experimental results quite well. At larger angles the DWBA distribution falls off more rapidly than observed experimentally, and it is interesting to note how dramatically the experimental angular distributions with  $\theta_{\text{c.m.}} > 30^\circ$  change with only a  $700$  keV change in bombarding energy. This rapid energy variation, along with the excitation function behavior, points to a breakdown of the assumption made in Refs. 1 and 2 of a purely direct reaction mechanism—an assumption which presupposes a slow variation of the reaction amplitudes as a function of energy.

### IV. BACKWARD-ANGLE MEASUREMENTS

The  $180^\circ$  excitation functions for both the ground and  $2^+$  states in  $^{28}\text{Si}$ , as seen in Fig. 4, are characterized by resonance structures with widths  $\Gamma \sim 1$  MeV and spacing comparable to the widths. For the ground-state excitation function there is further evidence of broader structures, not evident in the  $2^+$  excitation function, with widths  $\Gamma \sim 2-3$  MeV. There is some visual evidence of correlations in the intermediate structure in these two channels. Calculations of the cross-correlation coefficient for the two channels ( $C$ ) with data up to  $38$  MeV gives  $C = 0.38$ ;<sup>11</sup> with the full range of data the cross correlation increases to  $C = 0.45$ . As in Ref. 11, the experimental cross sections were averaged over intervals of  $900$  keV with the resulting cross sections placed on a grid of  $70$  equally spaced points,  $300$  keV apart (in Ref. 11 there

were 40 grid points). The cross correlation coefficient was then found using these generated excitation functions. The 70% confidence level of a true correlation, determined by an analysis of generated 70 point random spectra, corresponds to  $C=0.18$ . For perfect correlation,  $C=1$ .

The larger amount of structure observed in Fig. 4 for the  $180^\circ$  excitation function, as compared to the previously measured  $0^\circ$  excitation function shown in Fig. 2 by the open circles, may be ascribed to the relatively thicker target used in the latter measurement. When a thin target excitation function is measured at a forward angle,<sup>7</sup> intermediate structure more similar to that seen at backward angles is observed. In Fig. 5 the  $180^\circ$  excitation functions have been smoothed with an averaging interval of 1.3 MeV in order to make a reasonable comparison between the full range of  $0^\circ$  data and the  $180^\circ$  data. With this averaging the correlation between the  $0^+$  and  $2^+$  excitation functions is also more clearly evident—particularly for the higher energies,  $E_{c.m.} > 37$  MeV.

A feature of the backward angle data, which is also taken to indicate a resonance behavior, is that angular distributions measured at energies corresponding to maxima in the  $180^\circ$  excitation function can be reproduced well by a  $|P_l(\cos\theta)|^2$  angular dependence. This is shown in Fig. 6 for angular distributions obtained at the three backward angle maxima of  $E_{c.m.} = 27.8, 36.2,$  and  $45.7$  MeV. (The two lower energy distributions were first reported in Ref. 11). At each energy a  $|P_l(\cos\theta)|^2$  dependence has been fitted to the data and excellent agreement is observed. (In the simplest molecular model of two spinless particles orbiting each other, the relative orbital angular momentum  $l$  is just equal to the spin  $J$  of the molecular resonance.) The  $l$  values resulting in the best fits to these data are  $l=20, 26,$  and  $30$  at  $E_{c.m.} = 27.8, 36.2,$  and  $45.7$  MeV,

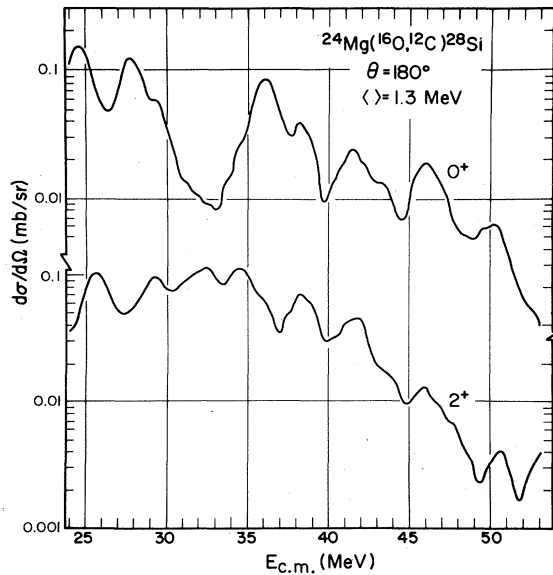


FIG. 5. The result of smoothing the data of Fig. 4 with an averaging interval of 1.3 MeV.

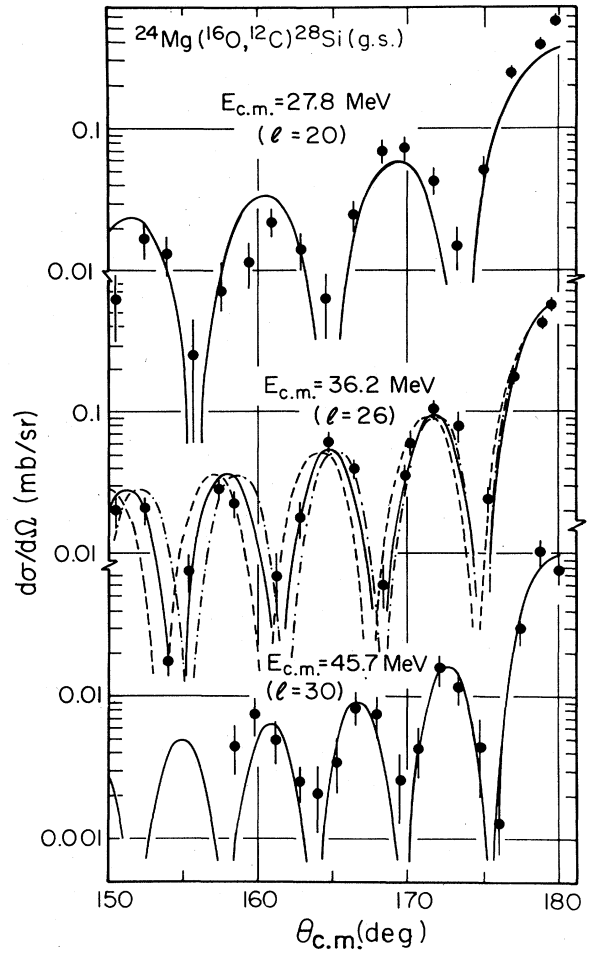


FIG. 6. Angular distributions at backward angles for the  $^{24}\text{Mg}(^{16}\text{O},^{12}\text{C})^{28}\text{Si}(\text{g.s.})$  reaction measured at  $E_{c.m.} = 27.8, 36.2,$  and  $45.7$  MeV. The curves represent  $|P_l(\cos\theta)|^2$  behavior, scaled to the data. The  $l$  values for the solid curves are indicated in the figure. The dashed curve is for  $l=25$ , and the dashed-dot curve is for  $l=27$ .

respectively. The quality of each fit is not substantially degraded by changing the  $l$  assignment by  $\pm 1$ , however. At 36.2 MeV curves for  $l=25$  (dotted) and  $l=27$  (dashed) are also shown. Later in the paper it will be indicated why an odd- $l$  assignment might be more appropriate at 36.2 MeV.

In Fig. 7,  $E_{c.m.}(^{16}\text{O}+^{24}\text{Mg})$  vs  $J(J+1)$  is plotted for the above three energies. The grazing angular momenta ( $l=J \approx kR$ ) in the entrance and exit channels are indicated schematically by the solid lines in the figure. These curves were obtained by calculating the absorption parameters  $\eta_l(E)$  at a number of energies using the optical potential of Erskine *et al.*,<sup>1</sup> and then determining the partial wave at each energy for which  $|\eta_l(E)| \approx 0.5$ . To within the uncertainties of the analysis, the angular momenta characterizing the backward angle structures seem to follow the grazing angular momentum.

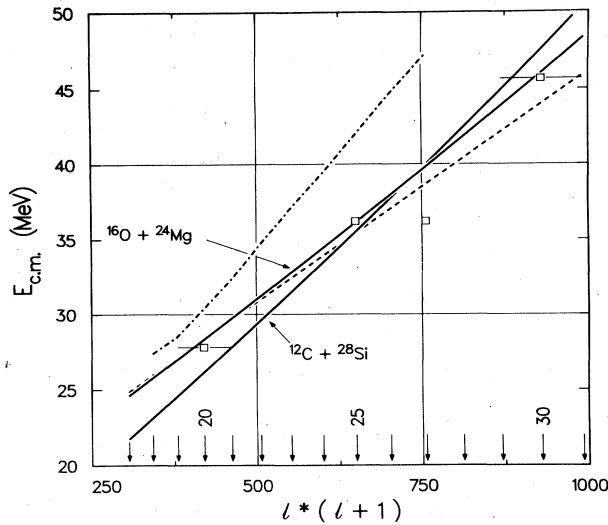


FIG. 7. Plot of  $E_{c.m.}$  ( $^{16}\text{O} + ^{24}\text{Mg}$ ) vs  $l(l+1)$  for the structures at  $E_{c.m.} = 27.8, 36.2,$  and  $45.7$  MeV. At  $36.2$  MeV we indicate by squares the preference for an odd- $l$  assignment, as discussed in the text. The solid curves represent the behavior of the grazing angular momentum in the entrance and exit channels. The dashed line shows the location of the rotational band used for the resonance analysis. The dotted curve represents the behavior of  $l_{\text{fus}}^{\text{max}}$ , as discussed in the text. The arrows at the bottom of the figure mark the locations of the  $l$  values from 17 to 31.

One general feature of the  $180^\circ$  data is that the average cross section remains relatively constant up to about  $E_{c.m.} \sim 35\text{--}40$  MeV, and then begins a rapid decline as the energy is further increased. A similar cross section falloff with energy has recently been observed in  $180^\circ$  elastic and inelastic scattering measurements for the  $^{16}\text{O} + ^{28}\text{Si}$  system.<sup>15</sup> In the present case the decline begins at approximately the same energy that the fusion cross section is found to reach its maximum value in the  $^{16}\text{O} + ^{24}\text{Mg}$  channel (at  $E_{c.m.} \sim 35$  MeV),<sup>19</sup> and a connection between these two effects seems possible.

The possibly diminishing influence of the fusion process with energy on the resonant partial wave over the energy range covered in the present paper is indicated in Fig. 7 by the dotted curve. This curve represents the maximum angular momentum contributing to fusion as a function of energy and was calculated using a sharp cutoff approximation for the fusion cross section (assuming that the lowest partial waves contribute to fusion):

$$\sigma_{\text{fus}} = \pi \lambda^2 (l_{\text{fus}}^{\text{max}} + 1)^2.$$

To obtain the dotted curve this expression was inverted for  $l_{\text{fus}}^{\text{max}}(E)$  using the measured  $^{16}\text{O} + ^{24}\text{Mg}$  fusion cross sections of Tabor *et al.*<sup>19</sup> The increasing separation between the curve for  $l_{\text{fus}}^{\text{max}}$  from the grazing angular momenta is a measure of the "saturation" of the fusion cross sections. Whereas, at  $E_{c.m.} = 27.8$  MeV the assignment of  $l = 20$  coincides with both the grazing angular momentum  $l_{\text{graz}}$  and  $l_{\text{fus}}^{\text{max}}$  within the uncertainties of the analysis, at higher energies the angular momenta observed in the reso-

nances are more nearly consistent with  $l_{\text{graz}}$ . If a more realistic behavior is assumed for the  $S$  matrix, then contributions to fusion will result from partial waves greater than  $l_{\text{fus}}^{\text{max}}$ . The saturation of the fusion cross section is assumed to be due to the fact that in the highest partial waves other processes, such as deep inelastic scattering, are becoming dominant. Since such processes occur on a faster time scale, they would therefore not show a resonant energy dependence.

## V. COMPARISON OF FORWARD AND BACKWARD ANGLE RESULTS

One of the surprises of the lower energy data<sup>11</sup> was the apparent lack of correlation between the  $0^\circ$  and  $180^\circ$  excitation functions. It is not difficult to understand how this can occur. In the  $^{24}\text{Mg}(^{16}\text{O}, ^{12}\text{C})^{28}\text{Si}$  transfer reaction, the direct alpha-transfer component is expected to dominate at forward angles. In terms of a partial wave decomposition of the differential cross section, where

$$\frac{d\sigma}{d\Omega} = \left| \sum_l \frac{1}{2ik_{\text{in}}} (2l+1) f_l P_l(\cos\theta) \right|^2,$$

the transition amplitudes  $f_l$  for a direct alpha-transfer process can be approximated using the DWBA, i.e.,  $f_l = f_l^{\text{DWBA}}$ . The highly oscillatory nature of the forward angle data indicates that only a few partial waves contribute strongly to the reaction and consequently limits the possible optical potentials which can be used to fit the data. To result in the observed behavior the DWBA amplitudes have to be strongly peaked about the grazing partial wave, with phases producing constructive interference at forward angles. This necessarily means that the backward angle cross section in DWBA will be very small. [This is reflected in the properties of the Legendre polynomials:  $P_l(\cos 0^\circ) = 1$ ;  $P_l(\cos 180^\circ) = (-1)^l$ .] For the  $^{24}\text{Mg}(^{16}\text{O}, ^{12}\text{C})^{28}\text{Si}(\text{g.s.})$  reaction, however, there is a fairly large yield at backward angles [ $(d\sigma/d\Omega)(180^\circ) \sim 0.01\text{--}0.1(d\sigma/d\Omega)(0^\circ)$ ], and further this yield is characterized by a single (or very few)  $l$  values.

The simplest modification to the transition amplitude which allows us to fit all of the observed features of the experimental cross section is to maintain  $f_l^{\text{DWBA}}$  as the background amplitude, but to introduce a resonance in one partial wave  $l'$  (where  $l' \approx l_{\text{graz}}$ ). Then  $f_l = f_l^{\text{DWBA}}$  for  $l \neq l'$  and  $f_{l'} = f_{l'}^{\text{DWBA}} + f_{l'}^{\text{res}}$ . In this manner enhanced backward angle yield is guaranteed, while the effect at forward angles depends on the relative phase of the DWBA and the added amplitude.

In Fig. 8 the angular distribution for the  $^{24}\text{Mg}(^{16}\text{O}, ^{12}\text{C})^{28}\text{Si}(\text{g.s.})$  reaction at  $E_{c.m.} = 36.2$  MeV covering most of the range from  $0^\circ$  to  $180^\circ$  is shown. Also shown is a fit where a DWBA background was assumed with a resonance contribution in the  $l = 27$  partial wave. As indicated earlier, when just the backward angle data are available, an  $l = 26$  assignment results in the best fit to these data. In the more complete angular distribution shown here, however, there is a deep minimum observed at  $90^\circ$ . This implies strength in an odd partial wave since  $P_{l,\text{odd}}(\cos 90^\circ) = 0$ . Similar results were obtained earlier in fitting another complete angular distribution at  $27.8$  MeV

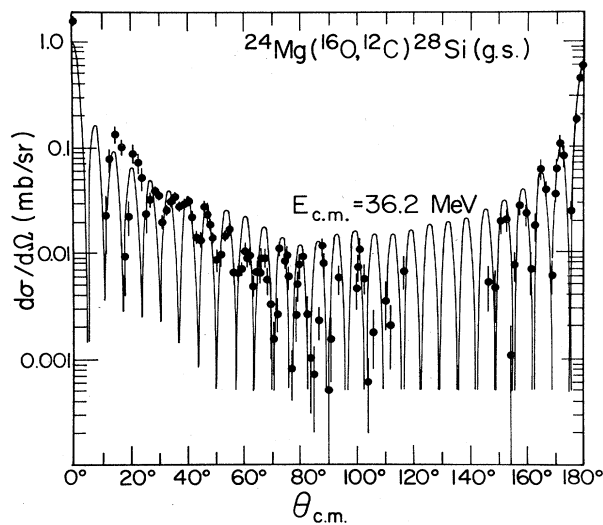


FIG. 8. Angular distribution for the  $^{24}\text{Mg}(^{16}\text{O}, ^{12}\text{C})^{28}\text{Si}(\text{g.s.})$  reaction measured at  $E_{\text{c.m.}} = 36.2$  MeV. The curve represents a fit to the data assuming a  $J=27$  resonance interfering with a direct-reaction DWBA amplitude as discussed in the text.

using the  $l=20$  assignment.<sup>4</sup> For the calculation in Fig. 8, as in the earlier calculation for the 27.8 MeV data, the DWBA background amplitudes were obtained using the optical model parameters of Ref. 1.

The energy dependence of the resonance amplitude  $f_l^{\text{res}}$  can be assumed to follow a Breit-Wigner behavior. Noting that the spacing of the resonance structure is comparable to the observed widths, it follows that the excitation functions must be characterized by at least partially overlapping resonances. An analysis of this kind has been found to be reasonably successful in fitting the data between 26 and 33 MeV (Ref. 5), where a DWBA background and two resonances at  $E_{\text{c.m.}} = 27.8$  and 30.8 MeV were assumed.

Where the data are sufficiently complete, this type of an analysis can establish reasonably model independent resonance parameters. In the earlier work the analysis included the  $0^\circ$  and  $180^\circ$  excitation functions and more complete angular distributions at a number of energies between 26 and 33 MeV. With only the  $0^\circ$  and  $180^\circ$  excitation functions to work with, it is impossible to perform a unique resonance analysis, although it can be hoped that the plausibility of different models can be established. In the next section the present data are discussed in the context of a molecular resonance picture.

## VI. RESONANCE ANALYSIS

In a molecular resonance description the structures would be interpreted as resulting from isolated or partially overlapping resonances, members of a rotational band in a highly deformed, clusterlike system. The configuration populated has to have a strong overlap with both the  $^{16}\text{O} + ^{24}\text{Mg}$  and  $^{12}\text{C} + ^{28}\text{Si}$  channels. For the  $0^\circ$  excitation function the interference between resonances and direct reaction background must also be considered. At present it is not clear how to determine within a molecular model

the relative phase  $\phi_{\text{rel}}$  of the resonant and background term.

The simplest resonance energy dependence would be the  $J(J+1)$  behavior for a rotational band. A simultaneous fit to the present  $0^\circ$  and  $180^\circ$  data was attempted using such a band of resonances with both parities present, assuming a Breit-Wigner energy dependence for the individual amplitudes. The band head energy  $E_0$  and moment of inertia  $\mathcal{I}$  were taken appropriate for an  $^{16}\text{O} + ^{24}\text{Mg}$  dimolecule as in Ref. 18 ( $\mathcal{I} = 7.05 \times 10^{-42}$  MeV s<sup>2</sup>,  $E_0 = 31.6$  MeV; see the dashed line in Fig. 7), and the relative phase angles, resonance amplitudes and one width (assumed constant for all resonances) were allowed to vary. A smooth background dependence was assumed at  $0^\circ$ . Rather than attempting to set this dependence with DWBA calculations—a procedure which has results that are very sensitive to the choice of optical model parameters—a 3rd order polynomial energy dependence was assumed for the background amplitude, with fitted coefficients. The background phase was assumed constant at  $0^\circ$ . (In DWBA calculations this phase varies slowly with energy.) For this analysis the  $0^\circ$  and  $180^\circ$  data were smoothed with an averaging interval of 1.3 MeV, and the  $180^\circ$  data have been scaled up by a factor of 3 to approximate the different angular averaging in the  $0^\circ$  and  $180^\circ$  measurements. This scaling factor was obtained by comparing small and large aperture measurements for the  $180^\circ$  yield at energies where angular distributions were measured. In Fig. 9 the results of the resonance analysis (also smoothed with an averaging interval of 1.3 MeV) are shown by the dashed curve. The dashed-dot curve through the  $0^\circ$  excitation function shows the behavior of the background used in the fit.

The fit to the already smoothed data shown in Fig. 9 was done varying 43 parameters (including the parameters associated with 19 resonances with spins between 17 and 35, inclusive). Clearly, undue emphasis should not be placed on the particular parameters obtained by this fit. Without additional angular distribution data, our approach should be viewed as being largely schematic, however, with 19 resonant poles of arbitrary amplitude and phase we can reproduce both the relative strength and the complexity of the  $\sim 8$  broader structures seen in the  $0^\circ$  to  $180^\circ$  excitation functions.

The total resonance width, assumed to be the same for each resonance, was found as  $\Gamma = 1.55$  MeV. The resonance reduced-width products  $\gamma_{\text{in}}\gamma_{\text{out}}(J)$  and phases  $\phi_{\text{rel}}(J)$  are plotted as functions of the resonance spin  $J$  in Fig. 10. The uncertainties shown in this figure are the diagonal elements of the error matrix. They indicate the change in each parameter which, if all of the other parameters are fixed at their “best” value, would result in the reduced chi-square,  $\chi^2/(\text{degree of freedom})$ , for the fit increasing by 1. The relative phases seem to have a smooth spin dependence. This regular behavior may indicate that the phases are determined by a simple dynamical feature of the interaction. There have been a number of attempts to describe the resonancelike behavior observed in large-angle elastic and inelastic scattering yields in terms of potential scattering or other parametrizations of the scattering matrix (see, for example, Refs. 20–24). This general

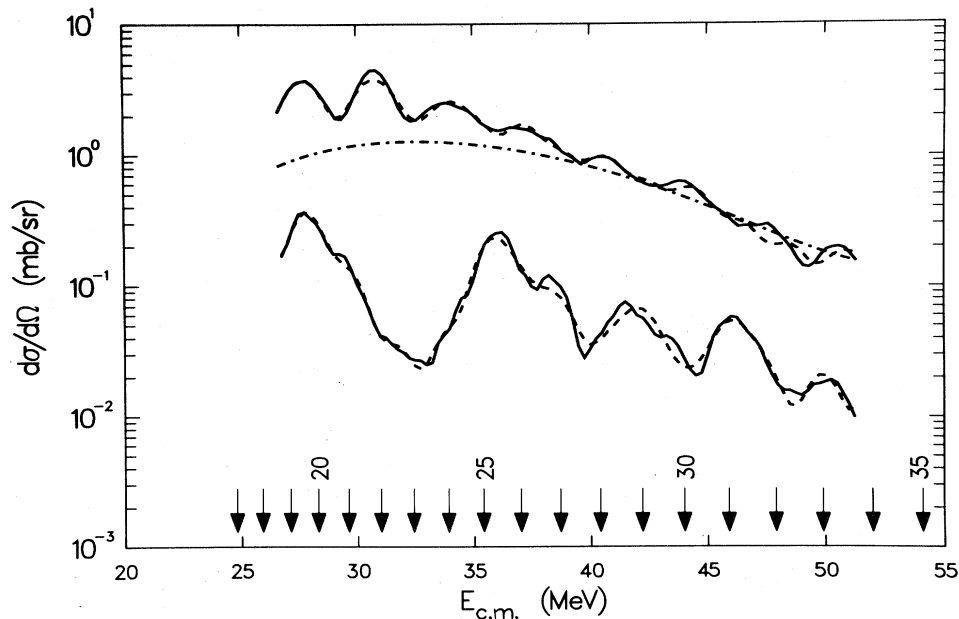


FIG. 9. The solid curves represent the  $\theta_{\text{lab}}=0^\circ$  and  $180^\circ$  excitation functions for the  $^{24}\text{Mg}(^{16}\text{O}, ^{12}\text{C})^{28}\text{Si}(\text{g.s.})$  reaction. These excitation functions have been smoothed with an averaging interval of 1.3 MeV. The  $180^\circ$  results have been scaled up by a factor of 3 to approximately account for the larger angular acceptance in these measurements. The dashed curves are the results of the resonance analysis discussed in the text. The dashed-dot curve indicates the direct-reaction background assumed at  $0^\circ$ . The arrows indicate the assumed resonance energies with  $17 \leq l_{\text{res}} \leq 35$ .

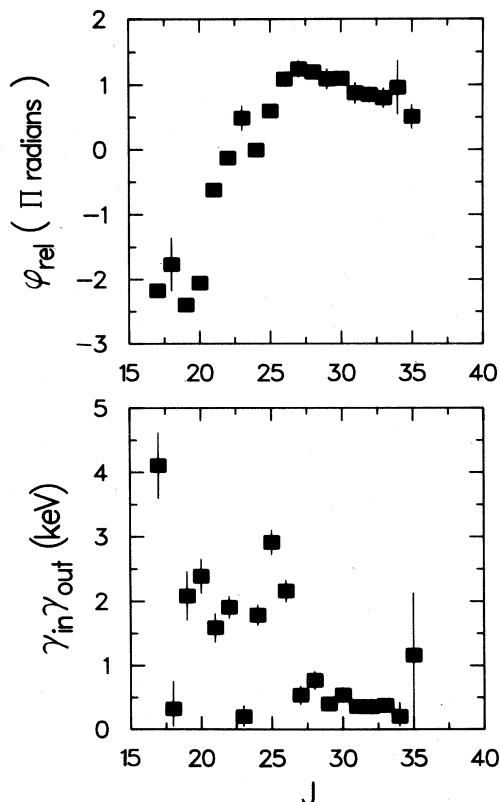


FIG. 10. The resonance phase angles and amplitudes as functions of spin ( $J=l_{\text{res}}$ ) obtained in the fit to the data. The error bars reflect the uncertainties obtained from the least squares fit under the assumption of a complete band of molecular resonances (see the text).

approach has been applied with some success by Robson and Smith<sup>25</sup> in describing the energy dependence of the  $^{24}\text{Mg}(^{16}\text{O}, ^{12}\text{C})^{28}\text{Si}(\text{g.s.})$  reaction by using exact finite-range DWBA calculations with a spin- and parity-dependent entrance channel potential. Our fitted resonance amplitudes do not have the regular behavior that the phases show and, with the  $J=18, 23,$  and  $27$  terms showing very small amplitudes compared to adjacent resonances, it appears that fitting the data actually requires fewer poles in the scattering amplitude than assumed in our simple band picture.

The surplus of terms in the band picture is not surprising when we compare the present results with our earlier analysis of the data between  $E_{\text{c.m.}}=26$  and  $33$  MeV.<sup>4</sup> In this region there are two strong peaks in the  $0^\circ$  excitation function located at  $E_{\text{c.m.}}=27.8$  and  $30.8$  MeV, although only the  $27.8$  MeV structure has a corresponding maximum in the  $180^\circ$  excitation function. The data used in the earlier analysis, consisting of excitation functions and angular distributions, were found consistent with having two resonances in this energy range at  $E_{\text{c.m.}}=27.8$  and  $30.8$  MeV, each of width  $800$  keV. The best fit to the data was obtained by spin assignments of  $J=20$  and  $J=23$  at these two energies, respectively.

## VII. SUMMARY AND CONCLUSIONS

Earlier measurements on the  $^{24}\text{Mg}(^{16}\text{O}, ^{12}\text{C})^{28}\text{Si}(\text{g.s.})$  reaction at both  $0^\circ$  and  $180^\circ$  have been extended to higher energies in order to investigate possible long range systematics in the observed resonance structures. These structures are found to persist to the highest energies measured in a remarkably uniform fashion, although their amplitudes decrease with increasing energy. The data

show some of the characteristics consistent with a band of resonances, although there are obvious gaps in the band.

The extension of the  $180^\circ$  excitation functions for both the  $^{28}\text{Si}(\text{g.s.})$  and  $^{28}\text{Si}(2^+, 1.78 \text{ MeV})$  states to higher energies indicates that the structures in the two channels are correlated at backward angles. This is in contrast to earlier measurements covering a more limited energy range where the  $0^\circ$  excitation functions for these two channels were shown to manifest correlated resonance structure, while the  $180^\circ$  excitation functions did not.

The interference effects which lead to the dissimilar excitation functions at  $180^\circ$  for the  $^{28}\text{Si}(\text{g.s.})$  and  $^{28}\text{Si}(2^+)$  states at lower energies points out the difficulty in analyzing

these reaction data. Small reaction cross sections make it very difficult to obtain the quality and quantity of data required to perform a quantitative resonance analysis in the presence of overlapping resonances. The present measurement and analysis indicate, however, that by increasing the body of available data, further systematics and simplicities in the resonance structures are likely to emerge.

This work was performed under the auspices of the U. S. Department of Energy, contract numbers DE-AC02-76ER03074 and W-31-109-ENG-38.

\*Present address: Physik-Department der Technischen Universität München, 8046 Garching, Federal Republic of Germany.

†Present address: Bell Telephone Company, Naperville, IL 60540.

‡Present address: Departement de Physique Nucléaire, Centre d'Etudes Nucléaires de Saclay, 91191 Gif-sur-Yvette Cedex, France.

<sup>1</sup>J. R. Erskine, W. Henning, D. G. Kovar, L. R. Greenwood, and R. M. DeVries, *Phys. Rev. Lett.* **34**, 680 (1975).

<sup>2</sup>J. C. Peng, J. V. Maher, W. Oelert, D. A. Sink, D. M. Cheng, and H. S. Song, *Nucl. Phys.* **A264**, 312 (1976).

<sup>3</sup>M. Paul, S. J. Sanders, J. Cseh, D. F. Geesaman, W. Henning, D. G. Kovar, C. Olmer, and J. P. Schiffer, *Phys. Rev. Lett.* **40**, 1310 (1978).

<sup>4</sup>S. J. Sanders, M. Paul, J. Cseh, D. F. Geesaman, W. Henning, D. G. Kovar, R. Kozub, C. Olmer, and J. P. Schiffer, *Phys. Rev. C* **21**, 1810 (1980).

<sup>5</sup>S. J. Sanders, C. Olmer, D. F. Geesaman, W. Henning, D. G. Kovar, M. Paul, and J. P. Schiffer, *Phys. Rev. C* **22**, 1914 (1980).

<sup>6</sup>J. Nurzynski, T. R. Ophel, P. D. Clark, J. S. Eck, D. F. Hebbard, P. C. Weisser, B. A. Robson, and R. Smith, *Nucl. Phys.* **A363**, 253 (1981).

<sup>7</sup>B. R. Fulton, J. B. A. England, S. D. Hoath, C. H. Atwood, and T. R. Ophel, *J. Phys. G* **8**, L141 (1982).

<sup>8</sup>P. Chevallier, D. Disdier, S. M. Lee, V. Rauch, G. Rudolf, and F. Scheibling, in *Proceedings of the International Conference on Nuclear Structure, Tokyo, 1977*, edited by the Organizing Committee (International Academic, Tokyo, 1977), p. 654.

<sup>9</sup>S. M. Lee, J. C. Adloff, P. Chevallier, D. Disdier, V. Rauch, and F. Scheibling, *Phys. Rev. Lett.* **42**, 429 (1979).

<sup>10</sup>M. R. Clover, B. R. Fulton, R. Ost, and R. M. DeVries, *J.*

*Phys. C* **5**, L63 (1979).

<sup>11</sup>M. Paul, S. J. Sanders, D. F. Geesaman, W. Henning, D. G. Kovar, C. Olmer, J. P. Schiffer, J. Barrette, and M. J. LeVine, *Phys. Rev. C* **21**, 1802 (1980).

<sup>12</sup>J. Barrette, M. J. LeVine, P. Braun-Munzinger, G. M. Berkowitz, M. Gai, J. W. Harris, and C. M. Jachcinski, *Phys. Rev. Lett.* **40**, 445 (1978).

<sup>13</sup>C. K. Gelbke, T. Awes, U. E. P. Berg, J. Barrette, M. J. LeVine, and P. Braun-Munzinger, *Phys. Rev. Lett.* **41**, 1778 (1978).

<sup>14</sup>J. Barrette, M. J. LeVine, P. Braun-Munzinger, G. M. Berkowitz, M. Gai, J. W. Harris, C. M. Jachcinski, and C. D. Ulhorn, *Phys. Rev. C* **20**, 1759 (1979).

<sup>15</sup>P. Braun-Munzinger *et al.* (unpublished).

<sup>16</sup>L. C. Northcliffe and R. F. Schilling, *Nucl. Data Tables* **7A**, 233 (1970).

<sup>17</sup>An attempt was made by Cindro and Pocanic (Ref. 18) to describe orbiting in the  $^{40}\text{Ca}$  system in this fashion. However, by their parameters a mean spacing of levels of only 1.7 MeV is found—approximately half of the observed spacing.

<sup>18</sup>N. Cindro and P. Pocanic, *J. Phys. G* **6**, 359 (1980).

<sup>19</sup>S. L. Tabor, D. F. Geesaman, W. Henning, D. G. Kovar, K. E. Rehm, and F. W. Prosser, Jr., *Phys. Rev. C* **17**, 2136 (1978).

<sup>20</sup>D. Dehnhard, V. Shkolnik, and M. A. Franey, *Phys. Rev. Lett.* **40**, 1549 (1978).

<sup>21</sup>S. Y. Lee, *Nucl. Phys.* **A311**, 518 (1978).

<sup>22</sup>S. Landowne, *Phys. Rev. Lett.* **42**, 633 (1979).

<sup>23</sup>S. Kubono, P. D. Bond, D. Horn, and C. E. Thorn, *Phys. Lett.* **84B**, 408 (1979).

<sup>24</sup>See also, P. Braun-Munzinger and J. Barrette, *Phys. Rep.* **87**, 209 (1982), and references therein.

<sup>25</sup>B. A. Robson and R. Smith, *Phys. Lett.* **123B**, 160 (1983).